# Irisin Attenuates Hepatic Stellate Cell Activation and Liver Fibrosis in Bile Duct Ligation Mice Model and Improves Mitochondrial Dysfunction

Thuy Linh Lai[1], So Young Park[1], Giang Nguyen[1], Phuc Thi Minh Pham[1], Seon Mee Kang[1], Jeana Hong[2], Jae-Ho Lee[3], Seung-Soon Im[3], Dae-Hee Choi[1], Eun-Hee Cho[1]

Departments of [1]Internal Medicine, [2]Pediatrics, Kangwon National University School of Medicine, Chuncheon; [3]Department of Physiology, Keimyung University School of Medicine, Daegu, Korea

**Background:** Liver fibrosis is a common outcome of chronic liver disease and is primarily driven by hepatic stellate cell (HSC) activation. Irisin, a myokine released during physical exercise, is beneficial for metabolic disorders and mitochondrial dysfunction. This study aimed to explore the effects of irisin on liver fibrosis in HSCs, a bile duct ligation (BDL) mouse model, and the associated mitochondrial dysfunction.

**Methods:** *In vitro* experiments utilized LX-2 cells, a human HSC line, stimulated with transforming growth factor-β1 (TGF-β1), a major regulator of HSC fibrosis, with or without irisin. Mitochondrial function was assessed using mitochondrial fission markers, transmission electron microscopy, mitochondrial membrane potential, and adenosine triphosphate (ATP) production. *In vivo*, liver fibrosis was induced in mice via BDL, followed by daily intraperitoneal injections of irisin (100 μg/kg/day) for 10 days.

**Results:** *In vitro*, irisin mitigated HSC activation and reduced reactive oxygen species associated with the TGF-β1/Smad signaling pathway. Irisin restored TGF-β1-induced increases in fission markers (Fis1, p-DRP1) and reversed the decreased expression of TFAM and SIRT3. Additionally, irisin restored mitochondrial membrane potential and ATP production lowered by TGF-β1 treatment. *In vivo*, irisin ameliorated the elevated liver-to-body weight ratio induced by BDL and alleviated liver fibrosis, as evidenced by Masson's trichrome staining. Irisin also improved mitochondrial dysfunction induced by BDL surgery.

**Conclusion:** Irisin effectively attenuated HSC activation, ameliorated liver fibrosis in BDL mice, and improved associated mitochondrial dysfunction. These findings highlight the therapeutic potential of irisin for the treatment of liver fibrosis.

**Keywords:** Liver cirrhosis; Irisin; Hepatic stellate cells; Mitochondria; Transforming growth factor beta1

## INTRODUCTION

Liver fibrosis is a wound-healing response triggered by diverse hepatic injuries, characterized by the excessive accumulation of extracellular matrix (ECM) due to the activation and proliferation of hepatic stellate cells (HSCs) [1]. Activated HSCs are the primary source of ECM in both parenchymal and cholestatic liver damage [2]. The progression of liver fibrosis stemming from chronic viral hepatitis, hepatotoxic substances, and liver diseases such as alcoholic or non-alcoholic fatty liver disease poses a significant threat to global public health. Therefore, investigating the fundamental causes of hepatic fibrosis is imperative.

HSC activation, driven by pro-fibrogenic cytokines including transforming growth factor-β (TGF-β) and connective tissue growth factor as well as platelet-derived growth factor-β, plays a pivotal role in hepatic fibrosis [3]. TGF-β stands out as a potent profibrotic cytokine, stimulating Smad signaling in HSCs and enhancing ECM synthesis [4]. Preventing TGF-β-induced HSC activation holds promise as a therapeutic approach for liver fibrosis.

Mitochondria are vital intracellular organelles that respond to cellular stress and metabolic changes. They serve as the primary energy source in hepatocytes, and their dysfunction is characteristic of various liver diseases [5,6]. Mitochondrial dysfunction is implicated in cholestatic liver damage and contributes to oxidative stress, inflammation, and cell death [7].

Experimental animal models, such as bile duct ligation (BDL), replicate features of secondary biliary fibrosis, making them invaluable for studying liver fibrosis [8,9]. BDL induces inflammatory liver damage and fibrosis in mice through obstructive cholestasis, providing a reliable time-dependent model for fibrosis induction with minimal variability [10]. Notably, BDL is a favorable method for inducing time-dependent fibrosis in mice, with minimal variability and mortality.

Irisin, discovered in 2012 as a myokine secreted from skeletal muscles, has garnered attention for its protective effects. Its levels rise following exercise, and it regulates various tissues and cells [11,12]. Studies have highlighted the protective role of irisin in cardiac, renal, pancreatic, and hepatic fibrosis [13-18]. Previous research from our team showed the ability of irisin to suppress HSC activation and reduce ECM deposition [19,20]. However, its effects on mitochondrial dysfunction and hepatic fibrogenesis remain unclear.

In this study, we explored the protective effects and molecular mechanisms of irisin in mitigating HSC activation and liver fibrosis induced by BDL as well as improving mitochondria dysfunction.

## METHODS

### Materials
The chemicals reagents used in the study were purchased from the following specified suppliers: recombinant human/murine/rat irisin from PeproTech Inc. (#100-65, Cranbury, NJ, USA); TGF-β1 from Bio-Techne (Minneapolis, MN, USA); Dulbecco's modified Eagle's medium (DMEM) from Welgene Inc. (Gyeongsan, Korea); penicillin-streptomycin from Life Technologies (Carlsbad, CA, USA); and fetal bovine serum from Access Cell Culture (Vista, CA, USA).

### Cell cultures
Immortalized human HSCs, LX-2 cells, were used and cells were cultured in DMEM supplemented with 10% fetal bovine serum and 100 U/mL penicillin/streptomycin. LX-2 cells were a gift from Professor Ja June Jang from Seoul National University (Korea). The passage number of LX-2 cells used in this research is under 30.

### Western blot analysis
LX-2 cells and liver tissue were lysed in radioimmunoprecipitation assay (RIPA) assay buffer (Atto Corporation, Tokyo, Japan). The protein concentration of total cell lysates was measured using a bicinchoninic acid (BCA) protein assay kit (Thermo Scientific Pierce, Rockford, IL, USA). Proteins from cell lysates were isolated using sodium dodecyl sulfate-polyacrylamide gel electrophoresis, transferred to a polyvinylidene fluoride membrane (Millipore, Billerica, MA, USA), and blocked with 5% bovine serum albumin or 5% nonfat dry milk for 1 hour at room temperature. Next, the membranes were washed three times with 1X Tris-buffered saline containing 0.5% Tween-20 (TBST) and incubated with primary antibodies overnight at 4°C or 2 hours at room temperature, following the manufacturer's instructions. After washing three times with TBST, the membranes were incubated with secondary antibodies for 2 hours at room temperature. Finally, the membranes were incubated with WestGlow PICO PLUS chemiluminescent substrate (Biomax, Seoul, Korea) and protein bands were detected using a ChemiDoc Imaging System (BioRad Laboratories Inc., Hercules, CA, USA). The developed protein bands were quantified using the ImageJ software (National Institute of Health, Bethesda, MD, USA).

Primary antibodies included α-smooth muscle actin (α-SMA),

superoxide dismutase 2 (SOD2), acetyl SOD2-K68 from Abcam (Cambridge, England); collagen type I (CO1A1) from Sigma-Aldrich (St. Louis, MO, USA); dynamin-related protein 1 (DRP1), phospho-DRP-1 (p-DRP1) (Serine 616), mitochondrial fission factor (MFF), phospho-MFF (p-MFF), sirtuin 3 (SIRT3), mitochondrial transcription factor A (TFAM), p-SMAD2, SMAD2, p-SMAD3, and SMAD3 from Cell Signaling Technology (Richmond, CA, USA); p-DRP1 (Serine 616) from Invitrogen (Waltham, MA, USA); fission protein 1 (Fis1) and succinate dehydrogenase subunit A (SDHA) from Santa Cruz Biotechnology (Dallas, TX, USA); and glyceraldehyde 3-phosphate dehydrogenase from GeneTex (Irvine, CA, USA).

## Measurement of reactive oxygen species level

LX-2 cells were seeded into 96-well microplates (20,000 cells per well). After 24 hours, cells were treated with TGF-β1 without or with irisin (10 or 20 nM) for 24 hours. Cells were washed and incubated with dichlorodihydrofluorescein diacetate (DCFDA) 2',7'–dichlorofluorescin diacetate (H2DCFDA; 20 μM) (ab113851, Abcam) for 45 minutes at 37°C in the dark. Images were obtained using a fluorescence microscope (Olympus, Tokyo, Japan), and the fluorescence intensity of immunostaining was quantified using ImageJ software.

## Transmission electron microscopy

LX-2 cells were seeded and treated with TGF-β1 (5 ng/mL), without or with irisin (10 or 20 nM) for 24 hours. Following incubation, the cells were fixed for 1 hour at 4°C in a solution of 2% paraformaldehyde and 2% glutaraldehyde with phosphate buffer pH 7.4, and then post-fixed for 40 minutes at 4°C with osmium tetroxide. The cells were dehydrated in graded concentrations of ethanol and treated with a graded propylene oxide series embedded in Epon. Each block was separated into ultrathin sections (80 nm), which were then placed on a copper grid. The samples were subsequently examined by transmission electron microscopy (JEOL-2100F, JEOL Ltd., Peabody, MA, USA; 200 kV) at the Korea Basic Science Institute in Chuncheon, Korea after staining with uranyl acetate and lead citrate.

## Measurement of malondialdehyde and adenosine triphosphate

Malondialdehyde (MDA) content was measured using a lipid peroxidation (MDA) assay kit (ab233471, Abcam). The reaction was based on the interaction between thiobarbituric acid and MDA, and absorbance was measured at 695 nm.

The adenosine triphosphate (ATP) content was measured using an ATP assay kit (No. ab83355, Abcam). LX-2 cells were harvested, washed with phosphate-buffered saline (PBS), and then resuspended in 100 μL of ATP assay buffer. Cells were homogenized and then centrifuged (13,000 g, 5 minutes, 4°C) to remove any insoluble material. Supernatants were collected and incubated with ATP probes. Absorbance was measured at 570 nm using a microplate reader.

## JC-1 mitochondrial membrane potential assay

Mitochondrial membrane potential (ΔψM) was assessed by using the JC-1 probe assay (ab113850, Abcam). LX- 2 cells were seeded at a density of 20,000 cells per well in black clear-bottom 96-well plates and incubated for 24 hours. Cells were stimulated with TGF-β1 and irisin 10 or 20 nM in culture medium without phenol red for 24 hours. After incubation, cells were washed with 1X PBS once, and incubated with 20 μM JC-1 in growing media without phenol red for 10 to 30 minutes at 37°C. The cells were then washed twice with 1X dilution buffer. The fluorescence intensity of the immunostaining was quantified using the ImageJ software.

## Animal experiments

This animal research protocol has been reviewed and approved by the Institutional Animal Care and Use Committee of Kangwon National University (KW-230323-1). Male C57BL/6J mice aged 6 to 8 weeks and weighing 18 to 20 g, were purchased from Doo Yeol Biotech (Seoul, Korea). All mice were housed under standard conditions of ambient temperature (22°C±1°C), with a 12-hour light/dark cycle and *ad libitum* access to water and food. All mice were acclimatized for 1 week before starting the experiment. The University Animal Care and Use Committee of Kangwon National University issued the protocols for animal experiments. To study BDL-induced liver fibrosis, mice were divided into three groups: sham (*n*=4), BDL (*n*=6), and BDL+irisin (*n*=7). Surgical procedures were performed under anesthesia and aseptic conditions. For sham operations, all steps were the same, except for the common BDL. Irisin (100 μg/kg/day) was dissolved in PBS and intraperitoneal injection immediately after surgery, once daily for a duration of 10 days. All animals were sacrificed 1 day after the last injection. Liver and blood were collected and preserved at –80°C for further analyses.

## Histological analysis of liver tissue samples

The liver tissue was fixed with formalin for 18 to 20 hours, embedded in paraffin, and cut into sections using a microtome (5 μm thick). For histological assessments using hematoxylin and

eosin staining, as well as Masson's trichrome staining, the sections were deparaffinized, rehydrated, and washed with distilled water. An Olympus microscope (TH4-200, Olympus) was used to examine the samples.

### Blood biochemistry analysis

Serum aspartate transaminase (AST) and alanine transaminase (ALT) levels were quantified using commercial enzyme kits (Asan Pharmaceutical, Seoul, Korea).

### Glycolytic extracellular acidification rate analysis

LX-2 cells were plated in XF24 cell culture microplates (Seahorse Bioscience, North Billerica, MA, USA) and treated with TGF-β1 (5 ng/mL), without or with irisin (10 or 20 nM) for 24 hours. Extracellular acidification rates (ECARs) were measured utilizing Agilent Seahorse XF analyzer (Agilent, Santa Clara, CA, USA) following to the manufacturer's protocol. Glycolysis

was assessed using the XF Glycolysis Stress Test kit according to the manufacturer's instructions.

### Statistical analyses

The results were presented as mean±standard error of mean from three independent experiments. Statistical analyses were performed using the GraphPad Prism 9 and 10 software 5 (GraphPad Software, San Diego, CA, USA). Statistical significance was set at $P < 0.05$.

## RESULTS

### Irisin suppressed TGF-β1-induced HSCs activation

In *in vitro* experiments, we first examined the anti-fibrotic potential of irisin in LX-2 cells. As depicted in Fig. 1A, irisin demonstrated a significant down-regulation of key fibrotic markers, including α-SMA and CO1A1, which were induced by TGF-β1.
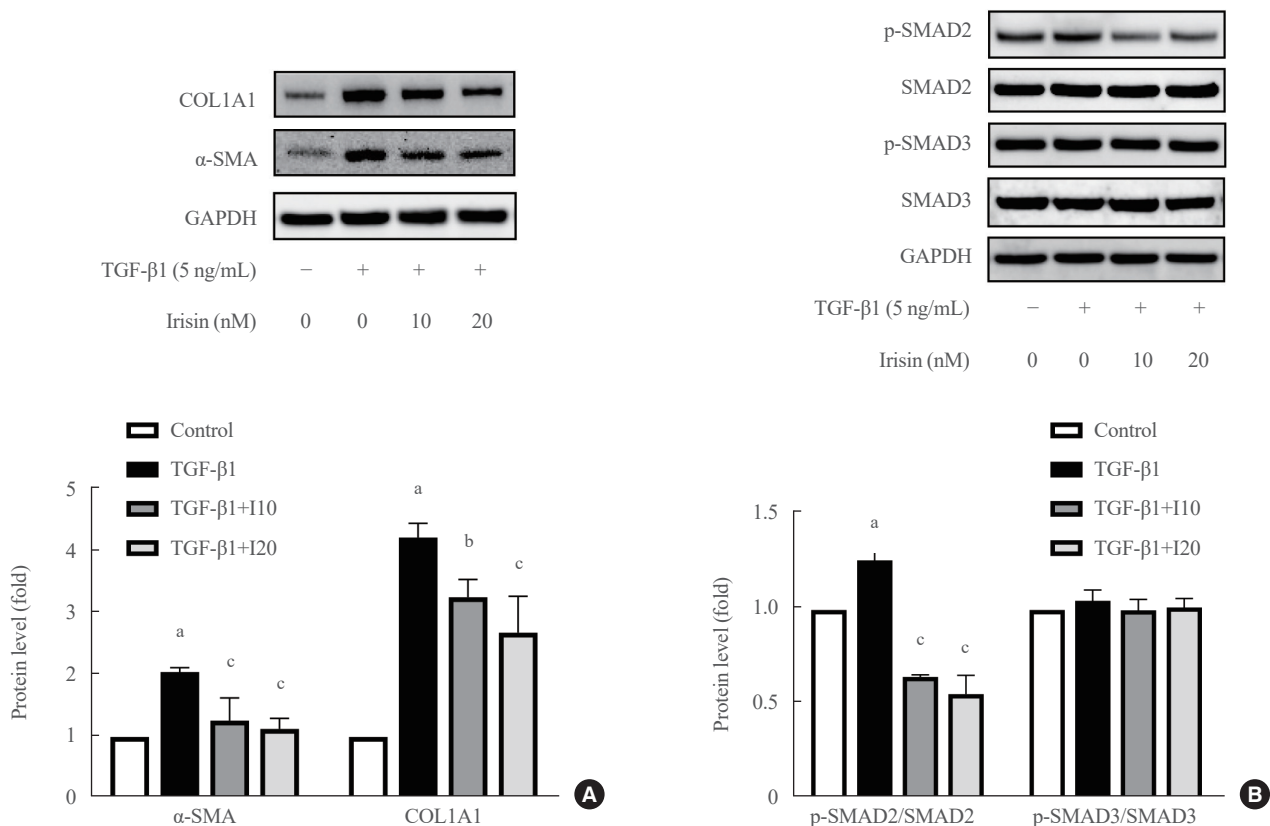


**Fig. 1.** Irisin suppressed transforming growth factor-β1 (TGF-β1)-induced hepatic stellate cells (HSCs) activation. LX-2 cells were treated with 5 ng/mL TGF-β1 and co-treated with 10 or 20 nM irisin for 24 hours. (A) Western blot analysis of α-smooth muscle actin (α-SMA) and collagen type 1 expression in LX-2 cells. (B) Western blot analysis of p-SMAD2, SMAD2, p-SMAD3, and SMAD3 expression in LX-2 cells. The quantitation of band intensities in Western blot images was calculated using ImageJ (National Institute of Health). The protein levels were normalized to glyceraldehyde 3-phosphate dehydrogenase (GAPDH) expression. All data are presented as mean±standard error of mean ($n \geq 3$). COL1A1, collagen type I alpha 1 chain. [a]$P < 0.01$ vs. control; [b]$P < 0.05$, [c]$P < 0.01$ vs. TGF-β1.

Furthermore, in Fig. 1B, irisin effectively attenuated the increased phosphorylation of SMAD2 induced by TGF-β1. These results strongly indicate that irisin exerts its anti-fibrotic effects by inhibiting the TGF-β1/SMAD2 signaling pathway. These findings hold promise for the therapeutic role of irisin in suppressing liver fibrosis and highlight its potential as a valuable candidate for further exploration in the treatment of hepatic fibrotic disorders.

## Irisin alleviated TGF-β1 induced reactive oxygen species and MDA production in HSCs

We investigated the effect of irisin on reactive oxygen species (ROS) production in LX-2 cells. ROS production contributes significantly to liver damage and the process of hepatic fibrogenesis [21]. As illustrated in Fig. 2A, the presence of TGF-β1 significantly elevated ROS levels in HSCs compared to the control. However, irisin treatment effectively mitigated the increase
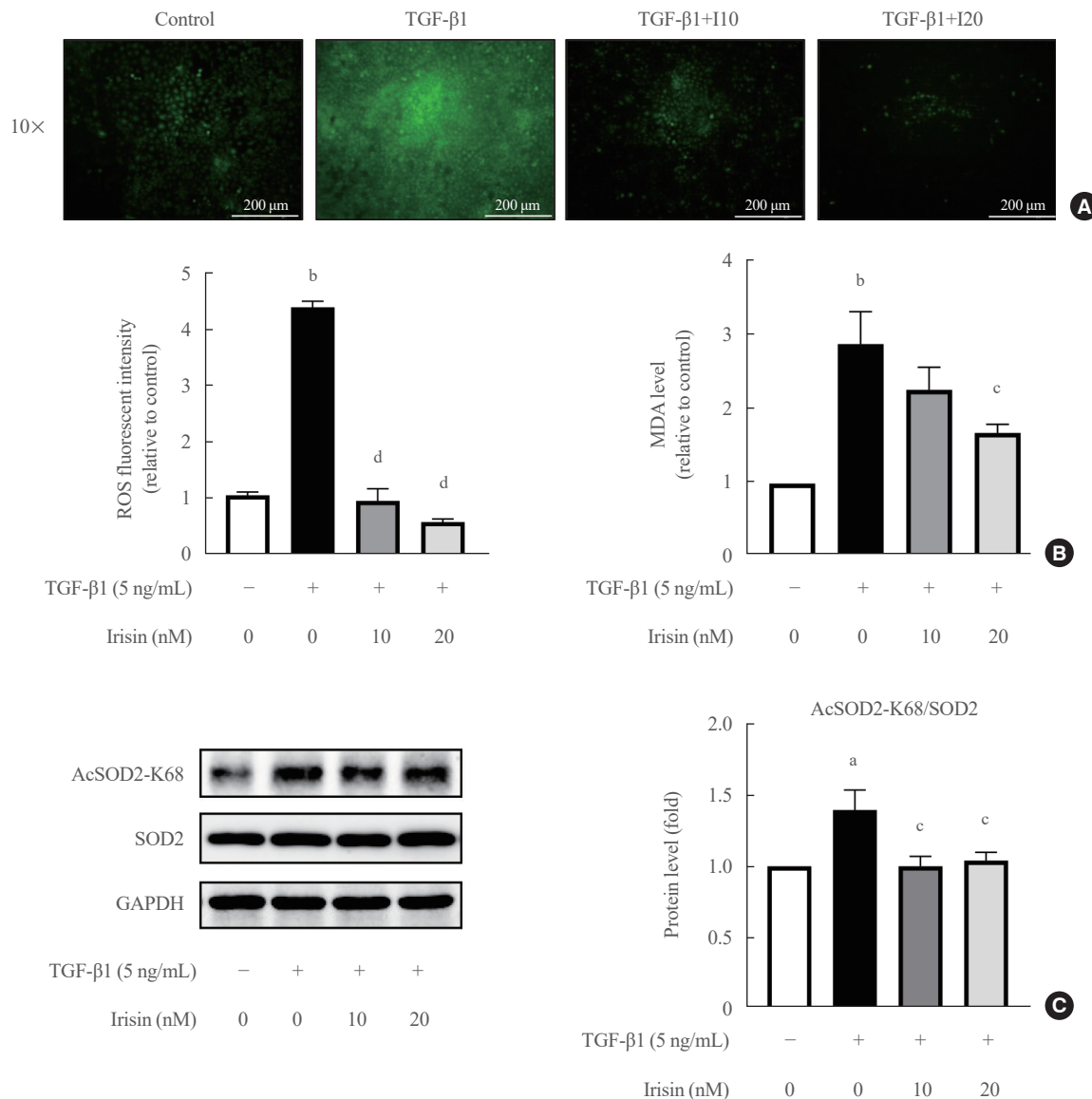
**Fig. 2.** Irisin alleviated transforming growth factor-β1 (TGF-β1)-induced reactive oxygen species (ROS) and malondialdehyde (MDA) production in hepatic stellate cells (HSCs). LX-2 cells were treated with 5 ng/mL TGF-β1 and co-treated with 10 or 20 nM irisin for 24 hours. (A) Cellular ROS by dichlorodihydrofluorescein diacetate (DCFDA) assay. The graph showing fluorescence intensity of immunostaining was quantified using ImageJ (National Institute of Health). (B) MDA level. (C) Western blot analysis of the expression of superoxide dismutase 2 (SOD2) acetylation on lysine 68 (acetyl superoxide dismutase2-K68 [AcSOD2-K68]) in LX-2 cells. The protein levels were normalized to glyceraldehyde 3-phosphate dehydrogenase (GAPDH) expression. All data are presented as mean±standard error of mean ($n \geq$ 3). [a]$P<0.05$, [b]$P<0.01$ vs. control; [c]$P<0.05$, [d]$P<0.01$ vs. TGF-β1.

in ROS production. This observation was further validated through the measurement of MDA levels, a well-known marker of oxidative stress, indicating a consistent trend (Fig. 2B). Additionally, we investigated the role of SOD2, a crucial enzyme that regulates mitochondrial ROS levels. Western blotting results revealed that TGF-β1 induced an increase in SOD acetylation at lysine 68. Importantly, irisin treatment counteracted this effect, as demonstrated in Fig. 2C. In summary, these results
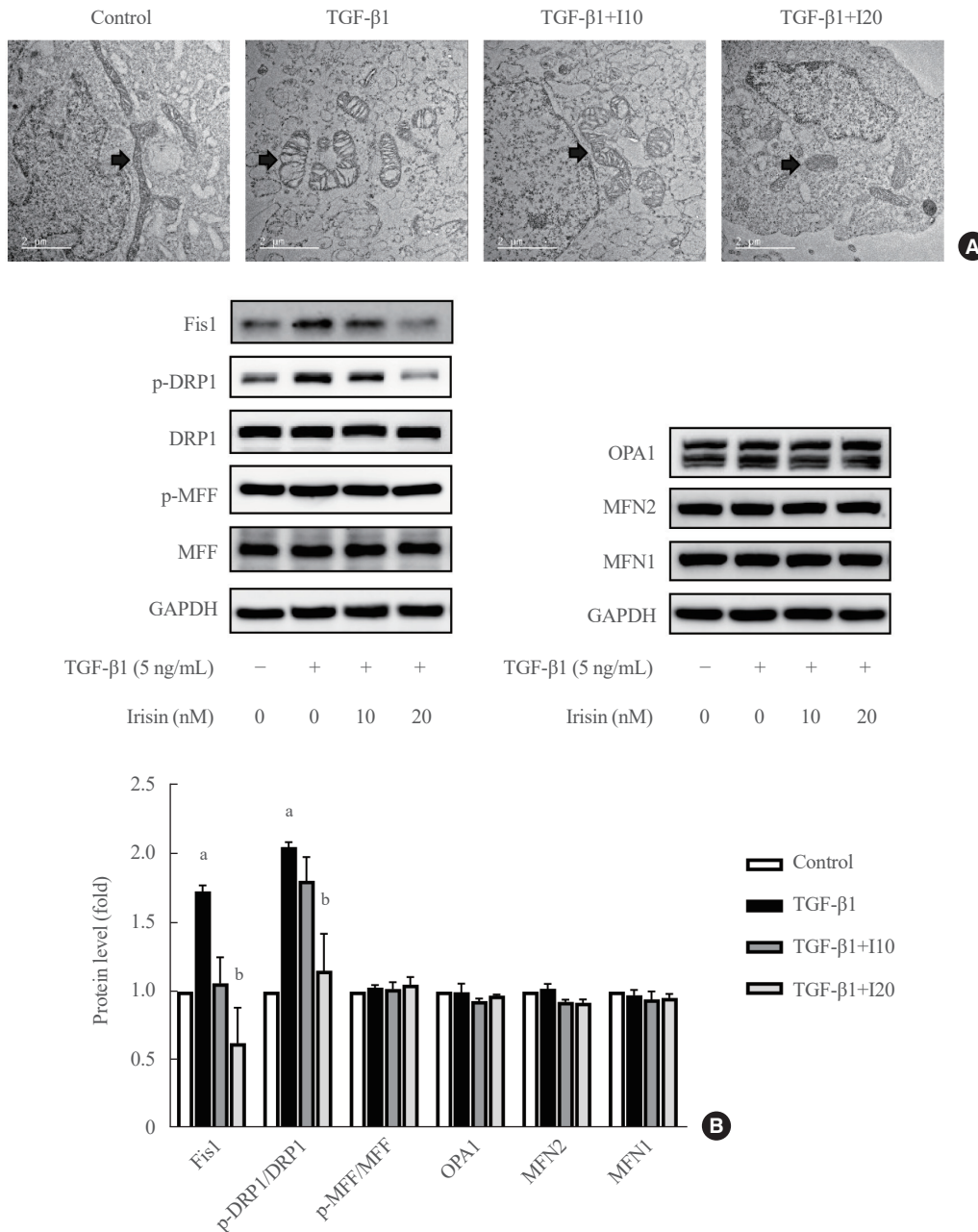


**Fig. 3.** Irisin attenuated transforming growth factor-β1 (TGF-β1)-induced mitochondrial fission in hepatic stellate cells (HSCs). LX-2 cells were treated with 5 ng/mL TGF-β1 and co-treated with 10 or 20 nM irisin for 24 hours. (A) Mitochondrial fission morphology was detected using transmission electron microscopy. Black arrows indicate mitochondria. (B) Western blot analysis of fission protein 1 (Fis1), phospho-dynamin-related protein 1 (p-DRP1), phospho-mitochondrial fission factor (p-MFF), total DRP1, total MFF, optic atrophy 1 (OPA1), mito-fusin 1 (MFN1), and mitofusin 2 (MFN2) expression in LX-2 cells. The quantitation of band intensities in Western blot images was calculated using ImageJ (National Institute of Health). The protein levels were normalized to glyceraldehyde 3-phosphate dehydrogenase (GAPDH) expression. All data are presented as mean±standard error of mean ($n \geq 3$). [a]$P < 0.05$, [b]$P < 0.01$ vs. control.

highlighted the protective effects of irisin against oxidative stress during HSC activation, emphasizing its potential therapeutic significance in the management of hepatic fibrosis-related oxidative damage.

**Irisin attenuated TGF-β1-induced mitochondrial fission in HSCs**

Next, we investigated the role of irisin in mitochondrial dynamics *in vitro*. We observed that under normal conditions, mitochondria displayed lengthy tubular forms, whereas TGF-β1 treatment showed an apparent alteration of mitochondrial morphology in transmission electron microscopy (Fig. 3A). The mitochondria were fissured into single mitochondrial units and swelling. However, irisin treatment reversed these effects and alleviated the mitochondrial morphology. In terms of protein

expression, markers associated with mitochondrial fission including p-DRP1 and mitochondrial Fis1 except p-MFF were significantly increased by stimulation with TGF-β1 and greatly suppressed by irisin treatment. Interestingly, the expression levels of mitochondrial fusion markers, including optic atrophy 1 (OPA1), mitofusin 1 (MFN1) and mitofusin 2 (MFN2) remained unchanged (Fig. 3B).

**Irisin alleviated TGF-β1-induced mitochondrial dysfunction in HSCs**

Next, we examined the protective effects of irisin on mitochondrial function. TFAM and SIRT3 protein were significantly decreased by TGF-β1; however, after irisin treatment, there was an evident rise of these two proteins (Fig. 4A). In addition, both ATP level and ΔΨm were notably lower in TGF-β1-activated
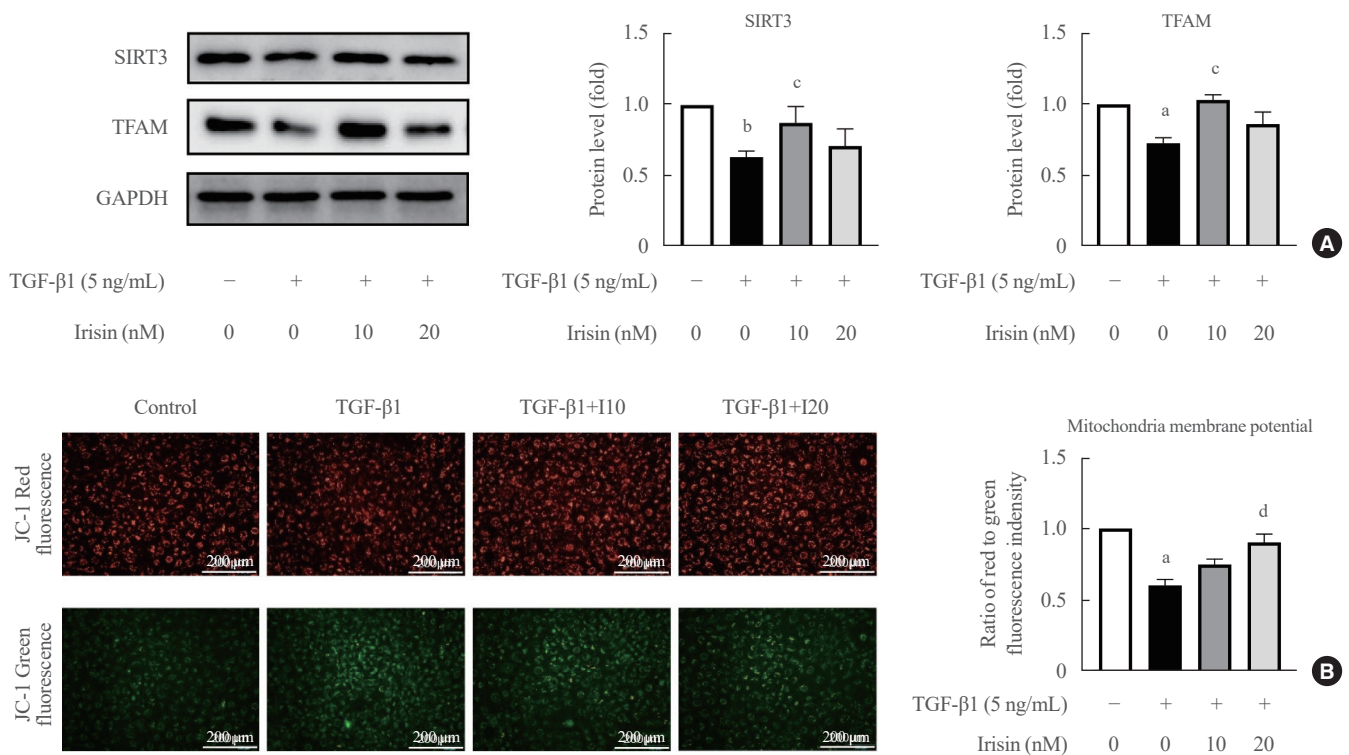


**Fig. 4.** Irisin alleviated transforming growth factor-β1 (TGF-β1)-induced mitochondrial dysfunction in hepatic stellate cells (HSCs). LX-2 cells were treated with 5 ng/mL TGF-β1 and co-treated with 10 or 20 nM irisin for 24 hours. (A) Western blot analysis of sirtuin 3 (SIRT3) and mitochondrial transcription factor A (TFAM) expression in LX-2 cells. (B) Mitochondrial membrane potential (ΔψM) was assessed using the JC-1 probe assay. The fluorescence intensity of immunostaining was quantified using ImageJ (National Institute of Health). (C) Adenosine triphosphate (ATP) production level in various groups of *in vitro* experiments. (D) Western blot analysis of succinate dehydrogenase subunit A (SDHA) expression in LX-2 cells. The quantitation of band intensities in Western blot images was calculated using ImageJ. The protein levels were normalized to glyceraldehyde 3-phosphate dehydrogenase (GAPDH) expression. All data are presented mean±standard error of mean ($n \geq 3$). (E) Seahorse analysis of extracellular acidification rate (ECAR), and glycolysis, glycolytic capacity and glycolytic reserve with 5 ng/mL TGF-β1 and co-treated with irisin (10 or 20 nM). Analysis of densitometry was performed and present data as the mean±standard error values of three independent experiments. OD, optical density; 2-DG, 2-deoxy-D-glucose. [a]$P<0.05$, [b]$P<0.01$ vs. control; [c]$P<0.05$, [d]$P<0.01$ vs. TGF-β1. *(Continued to the next page)*

HSCs compared to control and irisin administration reversed it (Fig. 4B, C). Protein levels of SDHA, an essential respiratory enzyme specific to mitochondrial complex II, were also increased by irisin treatment (Fig. 4D). The ECAR data indicated that treatment with TGF-β1 significantly increased glycolysis and treatment with irisin reduced glycolysis in LX-2 cells as indicated by the ECAR data (Fig. 4E).

Taken together, these results suggested that irisin has a protective effect against mitochondrial dysfunction in HSCs.

### Irisin improved BDL-induced liver injury and liver fibrosis in mice

The BDL procedure typically induces significant liver injury and severe hepatocellular damage. The morphology of the mice liver was observed to have a rougher appearance, including yellow dots, in the BDL groups compared with the sham groups,

and irisin treatment considerably improved these appearances (Fig. 5A). Furthermore, the liver weight-to-body weight ratio and serum levels of AST and ALT (Fig. 5B) were markedly increased in the BDL group, whereas animals receiving irisin injections had lower levels of these variables. Moreover, histopathological changes in the liver were analyzed by hematoxylin and eosin staining, which revealed that BDL treatment promoted cell infiltration, bile duct proliferation, and hepatocyte necrosis, whereas irisin improved these features. BDL treatment resulted in hepatic fibrosis, which was explained by the accumulation of collagen, whereas irisin improved these features as observed in Masson's trichrome staining (Fig. 5C). The protein levels of key fibrosis markers (α-SMA, collagen type I alpha 1 chain [COL1A1]), along with p-SMAD2, were also markedly reduced following irisin administration (Fig. 5D). These findings suggested that irisin alleviates liver fibrosis by suppressing
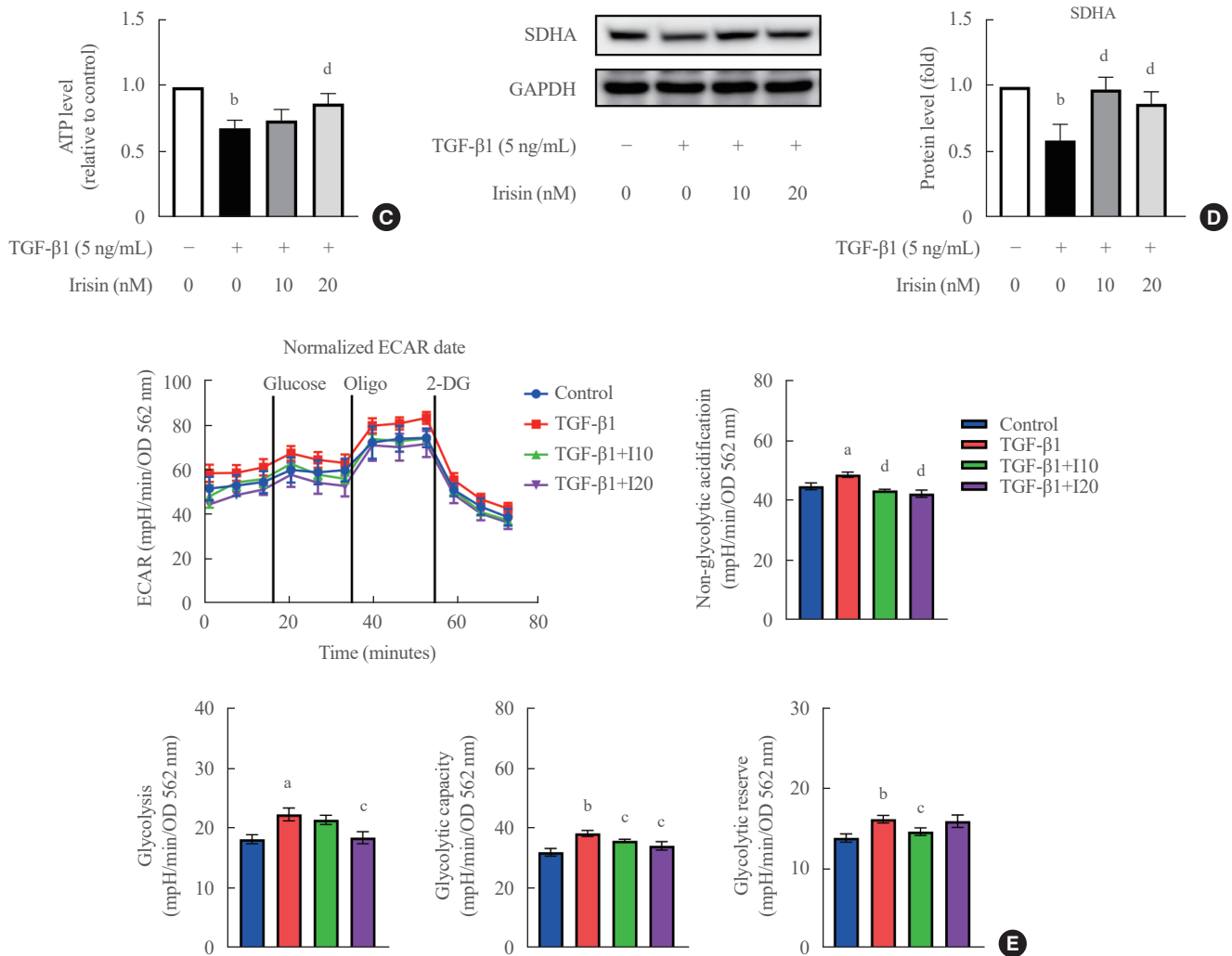


**Fig. 4.** Continued.
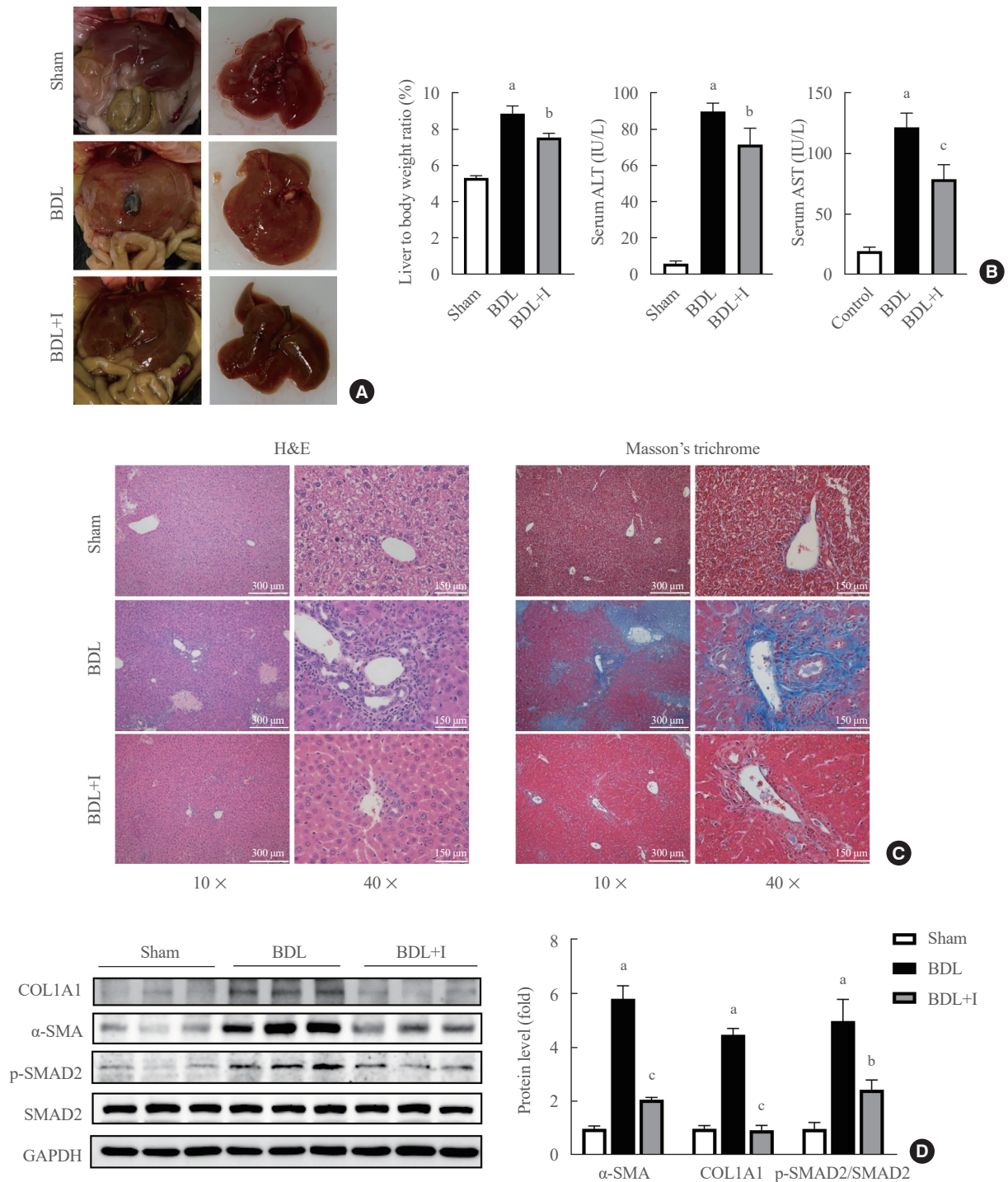
**Fig. 5.** Irisin improved bile duct ligation (BDL)-induced liver injury and liver fibrosis in mice. Mice underwent BDL to induce liver fibrosis. (A) Morphology of representative mice livers from the sham, BDL, and BDL+I groups. (B) The ratio of liver weight-to-body weight, serum alanine transaminase (ALT), and aspartate transaminase (AST) levels. (C) Sections of liver were stained with hematoxylin and eosin (H&E) staining; Masson's trichrome. The slides are magnified 10× and 40×. (D) Western blot analysis of α-smooth muscle actin (α-SMA), collagen type 1, p-SMAD2, and SMAD2 expression in liver from the sham, BDL, and BDL+I groups. The protein levels were normalized to glyceraldehyde 3-phosphate dehydrogenase (GAPDH) expression. All data are presented as mean±standard error of mean ($n \geq 3$). COL1A1, collagen type I alpha 1 chain. [a]$P < 0.05$, [b]$P < 0.01$ vs. sham group; [c]$P < 0.05$ vs. BDL group.

the TGF-β1/SMAD2 pathway in BDL models.

**Irisin recovered oxidative stress and mitochondrial dysfunction in BDL mice**

To confirm our *in vitro* results, we investigated the effects of iri-sin on oxidative stress and mitochondrial function in a BDL mice model. The level of acetyl-SOD2 and MDA, both indicative markers of oxidative stress, were higher in the BDL mice than in the sham group. However, irisin administration effectively lowered the levels of both these markers (Fig. 6A, B).
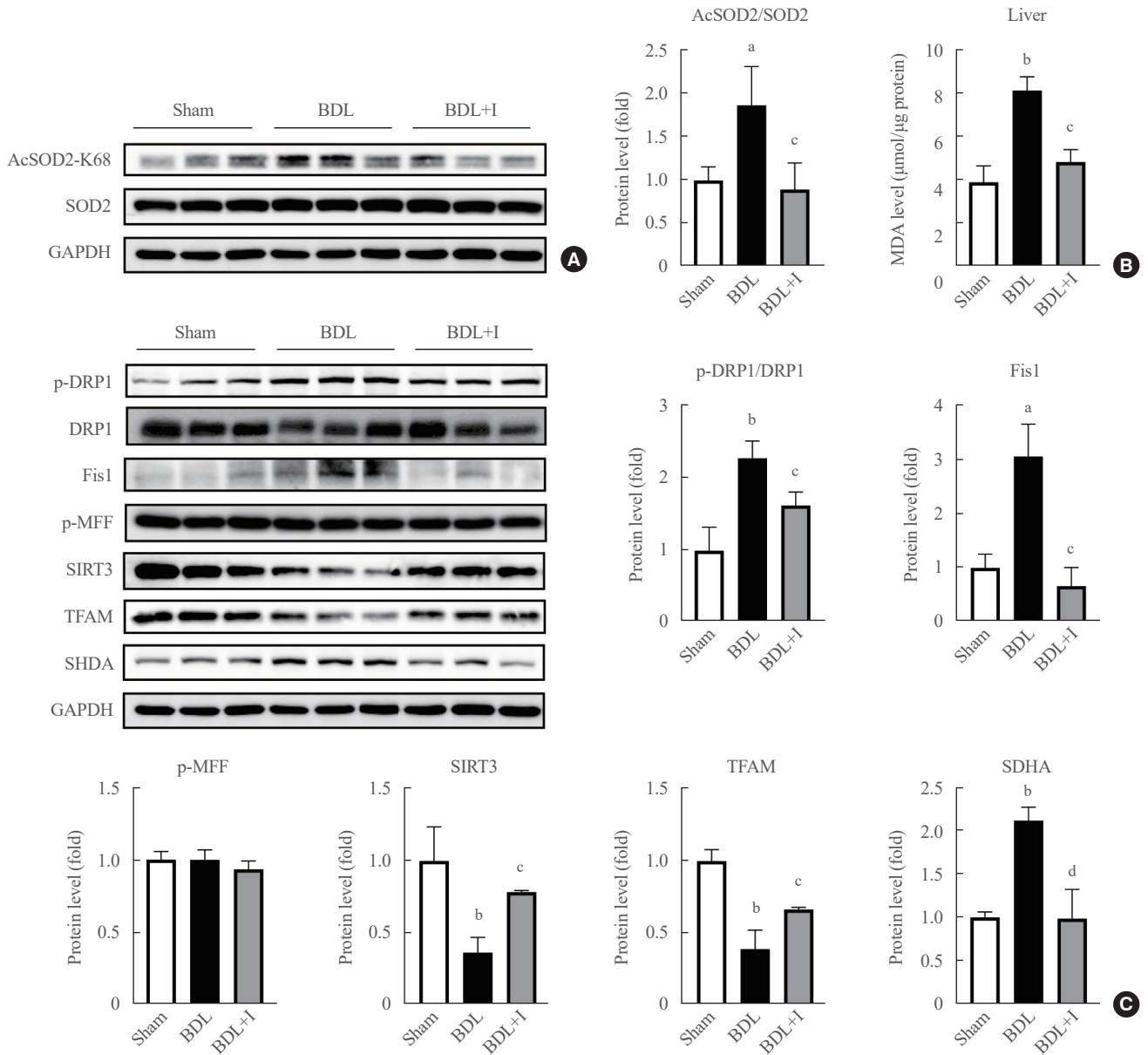


**Fig. 6.** Irisin recovered oxidative stress and mitochondrial dysfunction in bile duct ligation (BDL) mice. Irisin reversed the oxidative stress in the liver, as illustrated by the markers of oxidative stress. (A) The protein expression of acetyl superoxide dismutase 2-K68 (AcSOD2-K68) and (B) malondialdehyde (MDA) level. (C) Western blot analysis of fission protein 1 (Fis1), phospho-dynamin-related protein 1 (p-DRP1), phospho-mitochondrial fission factor (p-MFF), sirtuin 3 (SIRT3), mitochondrial transcription factor A (TFAM), and succinate dehydrogenase subunit A (SDHA) expression in liver. The quantitation of band intensities in Western blot images was calculated using ImageJ (National Institute of Health). The protein levels were normalized to glyceraldehyde 3-phosphate dehydrogenase (GAPDH) expression. All data are presented as mean±standard error of mean ($n≥3$). SOD2, superoxide dismutase 2; NS, no significance. [a]$P<0.05$, [b]$P<0.01$ vs. sham group; [c]$P<0.05$, [d]$P<0.01$ vs. BDL group.

Additionally, the results of the Western blot analysis were consistent with the *in vitro* data for irisin in the BDL model. These included mitochondrial fission markers (p-DRP1 and Fis1), markers associated with mitochondrial biogenesis (TFAM and SIRT3), and mitochondrial respiratory enzymes (SDHA) (Fig. 6C). Thus, our findings indicate that altered mitochondrial dysfunction, such as mitochondrial fission, may be involved in the protective effects of irisin against BDL-induced liver fibrosis.

## DISCUSSION

In this study, we successfully demonstrated the inhibitory effects of irisin on HSC activation *in vitro* and its ability to reduce liver fibrosis in an *in vivo* BDL-induced animal model. Notably, irisin exhibited a protective role by preserving both the morphological and functional integrity of mitochondria, which were otherwise compromised by the influence of TGF-β1 and BDL.

We also further investigated the signaling pathways involved in the biological effects of TGF-β1 in hepatic fibrosis. TGF-β1, a potent regulator in fibrogenesis, exerts its effects by activating downstream mediators, namely SMAD2 and SMAD3 [22]. Notably, our research revealed that irisin effectively mitigates TGF-β1-induced liver fibrosis in LX-2 cells by alleviating the phosphorylation of SMAD2, a critical component of the TGF-β1/SMAD2 signaling pathway. This compelling evidence not only validates the potential therapeutic efficacy of irisin but also identifies TGF-β1/SMAD2 signaling as a promising and specific target for interventions aimed at combating liver fibrosis.

Growing evidence indicates that HSC activation causes hepatic fibrosis and is often associated with mitochondrial dysfunction [23-25]. Many liver diseases, including steatohepatitis, cirrhosis, alcoholic liver disease, mitochondrial dysfunction, and oxidative stress are interconnected processes involving cell death, inflammation, and fibrosis [26]. In this study, we discovered that the fibrogenesis markers (α-SMA and CO1A1) and some of mitochondrial fission markers (the phosphorylation of Drp-1 and Fis1), as well as ROS production, were all increased in LX-2 cells by TGF-β1 treatment and in BDL mice model. Interestingly, irisin treatment counteracted these effects. It also attenuated TGF-β1 induced mitochondrial morphological changes, increased ATP production, and ΔψM. However, the pathways underlying this process have not yet been elucidated.

In terms of mitochondrial dynamics, the mitochondria within each cell undergo fusion and fission, which perform crucial functions in maintaining functional mitochondria when cells are exposed to metabolic or environmental stresses [27,28]. In our study, mitochondrial fusion markers remained unchanged, suggesting that irisin primarily influences mitochondrial fission rather than fusion. Numerous studies have demonstrated the therapeutic benefits of irisin in mitochondrial fission in various organs and other diseases [29-31].

Recent studies have shed light on irisin's mechanism of action through integrin αVβ5 in various tissues, including bone (osteocytes), white adipose tissue (adipocytes), and heart (cardiomyocytes) [32,33]. Specifically, in cardiomyocytes, irisin has been shown to mitigate mitochondrial fission, oxidative/nitrosative stress, and apoptosis through integrin αVβ5-protein kinase B (AKT)-dependent signaling pathways [33]. While our study did not investigate integrin αVβ5 in the liver or HSCs, future investigations will aim to elucidate its role in hepatocytes or HSCs.

In our study, irisin injection was found to reduce AST/ALT levels in mice with BDL induction. Several studies have highlighted irisin's hepatoprotective role, showing its ability to mitigate oxidative stress induced by palmitic acid in hepatocytes [34] and enhance autophagy in aged hepatocytes [35]. Recently, another study showed that administration of irisin attenuated liver fibrosis by reversing the release of fibrogenic extracellular vesicles from activated HSCs [36] suggesting the various target of irisin. However, the precise mechanisms underlying irisin's protective effects against liver injury or liver fibrosis remain elusive. Further investigations are warranted to elucidate these mechanisms.

Based on *in vitro* and *in vivo* investigations, we identified a protective role for irisin in the context of liver fibrosis. Nevertheless, the present study has some limitations. We have not yet clarified the precise signaling pathway between HSC activation and mitochondrial function. Irisin has been shown in previous studies to control body metabolism via the AMP-activated protein kinase (AMPK) and phosphoinositide 3-kinase (PI3K)/Akt [37,38]. To fully understand the therapeutic effects of irisin on liver fibrosis, further research is required to determine the mechanism by which irisin regulates mitochondrial dysfunction, both *in vitro* and *in vivo*.

In conclusion, the present study demonstrated that irisin mitigates HSC activation, ameliorates liver fibrosis in BDL mice, and improves mitochondrial dysfunction, revealing the strong potential of irisin as a valuable candidate for the development of effective liver fibrosis therapies. Further exploration and clinical studies in this direction hold significant promise for the advancement of liver disease treatment.

## CONFLICTS OF INTEREST

## ACKNOWLEDGMENTS

## AUTHOR CONTRIBUTIONS

Conception or design: D.H.C., E.H.C. Acquisition, analysis, or interpretation of data: T.L.L., S.Y.P., G.N., P.T.M.P., S.M.K., J.H., J.H.L., S.S.I. Drafting the work or revising: T.L.L. Final approval of the manuscript: E.H.C.

## ORCID

Thuy Linh Lai *https://orcid.org/0009-0001-2235-4972*
Eun-Hee Cho *https://orcid.org/0000-0002-1349-8894*
Dae-Hee Choi *https://orcid.org/0000-0002-8956-7518*

## REFERENCES

1. Bataller R, Brenner DA. Liver fibrosis. J Clin Invest 2005; 115:209-18.

2. Tsuchida T, Friedman SL. Mechanisms of hepatic stellate cell activation. Nat Rev Gastroenterol Hepatol 2017;14:397-411.

3. Pellicoro A, Ramachandran P, Iredale JP. Reversibility of liver fibrosis. Fibrogenesis Tissue Repair 2012;5(Suppl 1): S26.

4. Gressner AM, Weiskirchen R, Breitkopf K, Dooley S. Roles of TGF-beta in hepatic fibrosis. Front Biosci 2002;7:d793-807.

5. Han D, Ybanez MD, Johnson HS, McDonald JN, Mesropyan L, Sancheti H, et al. Dynamic adaptation of liver mitochondria to chronic alcohol feeding in mice: biogenesis, remodeling, and functional alterations. J Biol Chem 2012;287:42165-79.

6. Grattagliano I, Russmann S, Diogo C, Bonfrate L, Oliveira PJ, Wang DQ, et al. Mitochondria in chronic liver disease. Curr Drug Targets 2011;12:879-93.

7. Heidari R, Niknahad H. The role and study of mitochondrial impairment and oxidative stress in cholestasis. Methods Mol Biol 2019;1981:117-32.

8. Starkel P, Leclercq IA. Animal models for the study of hepatic fibrosis. Best Pract Res Clin Gastroenterol 2011;25:319-33.

9. Weiskirchen R, Weiskirchen S, Tag CG, Meurer SK. Induction of obstructive cholestasis in mice. Methods Mol Biol 2023;2669:163-75.

10. Tag CG, Sauer-Lehnen S, Weiskirchen S, Borkham-Kamphorst E, Tolba RH, Tacke F, et al. Bile duct ligation in mice: induction of inflammatory liver injury and fibrosis by obstructive cholestasis. J Vis Exp 2015;96:52438.

11. Bostrom P, Wu J, Jedrychowski MP, Korde A, Ye L, Lo JC, et al. A PGC1-α-dependent myokine that drives brown-fat-like development of white fat and thermogenesis. Nature 2012;481:463-8.

12. Korta P, Pochec E, Mazur-Bialy A. Irisin as a multifunctional protein: implications for health and certain diseases. Medicina (Kaunas) 2019;55:485.

13. Zhou B, Ling L, Zhang F, Liu TY, Zhou H, Qi XH, et al. Fibronectin type III domain-containing 5 attenuates liver fibrosis via inhibition of hepatic stellate cell activation. Cell Physiol Biochem 2018;48:227-36.

14. Peng H, Wang Q, Lou T, Qin J, Jung S, Shetty V, et al. Myokine mediated muscle-kidney crosstalk suppresses metabolic reprogramming and fibrosis in damaged kidneys. Nat Commun 2017;8:1493.

15. Chen RR, Fan XH, Chen G, Zeng GW, Xue YG, Liu XT, et al. Irisin attenuates angiotensin II-induced cardiac fibrosis via Nrf2 mediated inhibition of ROS/TGFβ1/Smad2/3 signaling axis. Chem Biol Interact 2019;302:11-21.

16. Ren Y, Zhang J, Wang M, Bi J, Wang T, Qiu M, et al. Identification of irisin as a therapeutic agent that inhibits oxidative stress and fibrosis in a murine model of chronic pancreatitis. Biomed Pharmacother 2020;126:110101.

17. Petta S, Valenti L, Svegliati-Baroni G, Ruscica M, Pipitone RM, Dongiovanni P, et al. Fibronectin type III domain-containing protein 5 rs3480 A>G polymorphism, irisin, and liver fibrosis in patients with nonalcoholic fatty liver disease. J Clin Endocrinol Metab 2017;102:2660-9.

18. Yang Z, Wei J, Wang Y, Du Y, Song S, Li J, et al. Irisin ameliorates renal tubulointerstitial fibrosis by regulating the Smad4/β-catenin pathway in diabetic mice. Diabetes Metab Syndr Obes 2023;16:1577-93.

19. Do DV, Park SY, Nguyen GT, Choi DH, Cho EH. The effects of irisin on the interaction between hepatic stellate cell

and macrophage in liver fibrosis. Endocrinol Metab (Seoul) 2022;37:620-9.

20. Dong HN, Park SY, Le CT, Choi DH, Cho EH. Irisin regulates the functions of hepatic stellate cells. Endocrinol Metab (Seoul) 2020;35:647-55.

21. Sanchez-Valle V, Chavez-Tapia NC, Uribe M, Mendez-Sanchez N. Role of oxidative stress and molecular changes in liver fibrosis: a review. Curr Med Chem 2012;19:4850-60.

22. Lai KN, Tang SCW. Diabetes and the kidney. Basel: S.Karger AG; 2011. Chapter 9, Transforming growth factor-β and Smads; p. 75-82.

23. Li X, Zhang W, Cao Q, Wang Z, Zhao M, Xu L, et al. Mitochondrial dysfunction in fibrotic diseases. Cell Death Discov 2020;6:80.

24. Middleton P, Vergis N. Mitochondrial dysfunction and liver disease: role, relevance, and potential for therapeutic modulation. Therap Adv Gastroenterol 2021;14:17562848211031394.

25. Nguyen G, Park SY, Do DV, Choi DH, Cho EH. Gemigliptin alleviates succinate-induced hepatic stellate cell activation by ameliorating mitochondrial dysfunction. Endocrinol Metab (Seoul) 2022;37:918-28.

26. Mansouri A, Gattolliat CH, Asselah T. Mitochondrial dysfunction and signaling in chronic liver diseases. Gastroenterology 2018;155:629-47.

27. Kadenbach B. Mitochondrial oxidative phosphorylation: nuclear-encoded genes, enzyme regulation, and pathophysiology. New York: Springer; 2012. Chapter 2, Mitochondrial dynamics: the intersection of form and function; p. 13-40.

28. Bi J, Zhang J, Ren Y, Du Z, Li Q, Wang Y, et al. Irisin alleviates liver ischemia-reperfusion injury by inhibiting excessive mitochondrial fission, promoting mitochondrial biogenesis and decreasing oxidative stress. Redox Biol 2019;20:296-306.

29. Tan Y, Ouyang H, Xiao X, Zhong J, Dong M. Irisin ameliorates septic cardiomyopathy via inhibiting DRP1-related mitochondrial fission and normalizing the JNK-LATS2 sig-

naling pathway. Cell Stress Chaperones 2019;24:595-608.

30. Wang PW, Pang Q, Zhou T, Song XY, Pan YJ, Jia LP, et al. Irisin alleviates vascular calcification by inhibiting VSMC osteoblastic transformation and mitochondria dysfunction via AMPK/Drp1 signaling pathway in chronic kidney disease. Atherosclerosis 2022;346:36-45.

31. Rabiee F, Lachinani L, Ghaedi S, Nasr-Esfahani MH, Megraw TL, Ghaedi K. New insights into the cellular activities of Fndc5/Irisin and its signaling pathways. Cell Biosci 2020;10:51.

32. Kim H, Wrann CD, Jedrychowski M, Vidoni S, Kitase Y, Nagano K, et al. Irisin mediates effects on bone and fat via αV integrin receptors. Cell 2018;175:1756-68.

33. Lin C, Guo Y, Xia Y, Li C, Xu X, Qi T, et al. FNDC5/irisin attenuates diabetic cardiomyopathy in a type 2 diabetes mouse model by activation of integrin αV/β5-AKT signaling and reduction of oxidative/nitrosative stress. J Mol Cell Cardiol 2021;160:27-41.

34. Park MJ, Kim DI, Choi JH, Heo YR, Park SH. New role of irisin in hepatocytes: the protective effect of hepatic steatosis in vitro. Cell Signal 2015;27:1831-9.

35. Bi J, Yang L, Wang T, Zhang J, Li T, Ren Y, et al. Irisin improves autophagy of aged hepatocytes via increasing telomerase activity in liver injury. Oxid Med Cell Longev 2020;2020:6946037.

36. Liao X, Luo Y, Gu F, Song W, Nie X, Yang Q. Therapeutic role of FNDC5/irisin in attenuating liver fibrosis via inhibiting release of hepatic stellate cell-derived exosomes. Hepatol Int 2023;17:1659-71.

37. Liu TY, Shi CX, Gao R, Sun HJ, Xiong XQ, Ding L, et al. Irisin inhibits hepatic gluconeogenesis and increases glycogen synthesis via the PI3K/Akt pathway in type 2 diabetic mice and hepatocytes. ClinSci (Lond) 2015;129:839-50.

38. Zhang D, Xie T, Leung PS. Irisin ameliorates glucolipotoxicity-associated β-cell dysfunction and apoptosis via AMPK signaling and anti-inflammatory actions. Cell Physiol Biochem 2018;51:924-37.